

# Methods for Measuring Rates of Protein Binding to Insoluble Scaffolds in Living Cells: Histone H1-Chromatin Interactions

Tanmay Lele,<sup>1</sup> Stefan R. Wagner,<sup>2</sup> Jeffrey A. Nickerson,<sup>2</sup> and Donald E. Ingber<sup>1\*</sup>

<sup>1</sup>Vascular Biology Program, Departments of Pathology and Surgery, Children's Hospital, Harvard Medical School, Boston, Massachusetts

<sup>2</sup>Department of Cell Biology and Cancer Center, University of Massachusetts Medical School, Worcester, Massachusetts

**Abstract** Understanding of cell regulation is limited by our inability to measure molecular binding rates for proteins within the structural context of living cells, and many systems biology models are hindered because they use values obtained with molecules binding in solution. Here, we present a kinetic analysis of GFP-histone H1 binding to chromatin within nuclei of living cells that allows both the binding rate constant  $k_{\text{ON}}$  and dissociation rate constant  $k_{\text{OFF}}$  to be determined based on data obtained from fluorescence recovery after photobleaching (FRAP) analysis. This is accomplished by measuring the ratio of bound to free concentration of protein at steady state, and identifying the rate-determining step during FRAP recovery experimentally, combined with mathematical modeling. We report  $k_{\text{OFF}} = 0.0131/\text{s}$  and  $k_{\text{ON}} = 0.14/\text{s}$  for histone H1.1 binding to chromatin. This work brings clarity to the interpretation of FRAP experiments and provides a way to determine binding kinetics for nuclear proteins and other cellular molecules that interact with insoluble scaffolds within living cells. *J. Cell. Biochem.* 99: 1334–1342, 2006. © 2006 Wiley-Liss, Inc.

**Key words:** FRAP; nuclear; photobleaching; mathematical model; scaffold; histone; binding

Our understanding of cell form and function is largely based on static images. Yet virtually, all cellular structures undergo continual turnover in which individual molecules can diffuse throughout the cytoplasm, and bind and unbind to other soluble molecules, as well as to larger insoluble scaffolds in the cytoplasm and nucleus. Because analysis of molecular binding interactions is difficult in whole cells, most of our knowledge of molecular binding rates is based on studies with isolated components

carried out in solution, and these are the rates used in most systems biology models of cell regulation. But many cellular proteins normally function when bound to insoluble molecular scaffolds, such as signaling complexes, cytoskeletal filaments, chromatin, and the nuclear matrix that appear beneath the surface membrane, in the cytoplasm, or within the nucleus [Ingber, 1993; Nickerson, 2001; Zink et al., 2004]. It is therefore crucial to be able to determine the binding rates for these molecules in the physiological context of living cells.

Analysis of molecular binding interactions can be carried out in living cells expressing proteins that are labeled with fluorescent dyes or tagged with green fluorescent protein (GFP), in combination with the fluorescence recovery after photobleaching (FRAP) technique. In FRAP, fluorescently labeled molecules within a small region of the surface membrane, cytoplasm, or nucleus are exposed to a brief pulse of laser irradiation that bleaches molecules within the path of the beam without altering their structure or function. Repeated fluorescence images of the bleached zone can be

Grant sponsor: NIH; Grant number: CA-45548; Grant sponsor: NSF grant; Grant number: DMR-0213805; Grant sponsor: American Cancer Society; Grant number: RSG 99-262-04; Grant sponsor: National Cancer Institutes; Grant number: PO1 CA82834.

\*Correspondence to: Donald E. Ingber, MD, PhD, Vascular Biology Program, KFRL 11.127, Children's Hospital, 300 Longwood Avenue, Boston, MA 02115.

E-mail: donald.ingber@childrens.harvard.edu

Received 25 October 2005; Accepted 19 April 2006

DOI 10.1002/jcb.20997

© 2006 Wiley-Liss, Inc.

used to measure the rate at which fluorescent molecules redistribute and replace photo-bleached ones. Most papers in the biological literature, however, only report the data in terms of the half time of recovery measured over several minutes. Others report “apparent” diffusion coefficients, even though FRAP recovery may be limited by binding and not by diffusion depending on the experimental conditions. Thus, the need for a better interpretation and mathematical analysis of FRAP data has become clear [Kaufman and Jain, 1990, 1991; Lele et al., 2004; Sprague et al., 2004; Sprague and McNally, 2005]. This is particularly true for nuclear proteins which can exhibit complex binding dynamics with insoluble chromatin or nuclear matrix [Koppel and Sheetz, 1983; Kaufman and Jain, 1990, 1991; Tardy et al., 1995; Phair and Misteli, 2000, 2001; Stenoien et al., 2001, 2002; Presley et al., 2002; Carrero et al., 2003; Karpova et al., 2004; Lele et al., 2004; Phair et al., 2004a, 2004b; Sprague et al., 2004; Hinojos et al., 2005].

In the present study, we focus on the development of a method to measure the binding and unbinding rate constants ( $k_{\text{ON}}$  and  $k_{\text{OFF}}$ , respectively) for histone H1 protein to chromatin within nuclei of living cells. Chromatin structure is highly complex as almost 2 m of DNA are packaged into a nucleus with a typical diameter of 10  $\mu\text{m}$  in human cells. The first level of packaging is the nucleosome, formed by the wrapping of DNA around a nucleosomal core consisting of an octamer complex with two molecules each of histones H2A, H2B, H3, and H4 [Luger et al., 1997; Richmond et al., 1984]. This forms a chromatin structure that appears as “beads on a string” when viewed in an electron microscope [Olins and Olins, 1974]. Histone H1 binds to 23 base pairs of DNA that extend out from this nucleosomal core [Travers, 1999]. Binding of histone H1 facilitates further folding of the nucleosomal strings into more condensed chromatin structures; this represses transcription, and the release of histone H1 from internucleosomal DNA-binding sites may be an important step in the activation of gene transcription [Zlatanova et al., 2000]. Binding of histone H1 to DNA has been characterized in vitro [Mamoon et al., 2005]; however, the relevance of these results for understanding kinetics of histone exchange with binding sites on DNA within intact chromatin in living cells remains unclear. Histone H1 is also a good

choice for this analysis because it is abundant and widely distributed in the nucleus, it binds to specific DNA sequences through a simple bimolecular interaction [Wolffe, 1998] and, unlike the nucleosomal core histones, it does not bind to DNA as part of a larger multi-protein complex. In addition, the binding and unbinding of histone H1 to DNA is likely to be altered in much simpler ways than the complicated mechanisms by which whole nucleosomes are “remodeled” [Imbalzano and Xiao, 2004].

Past studies have shown that when molecular diffusion is much faster than both binding and unbinding rates, FRAP recovery depends only on  $k_{\text{OFF}}$ , and not  $k_{\text{ON}}$  [Kaufman and Jain, 1991; Bulinski et al., 2001; Lele et al., 2004]. Based on this observation, the FRAP method can be modified to determine the  $k_{\text{OFF}}$  of certain proteins within living cells [Lele and Ingber, 2005; Lele et al., 2005]. But an independent experimental technique is needed to reliably estimate  $k_{\text{ON}}$ . Here, we present a new method to estimate  $k_{\text{ON}}$  by measuring the ratio of bound to free concentration of protein at steady state in living cells; this ratio is equal to  $k_{\text{ON}}/k_{\text{OFF}}$ . We further present a method to identify the rate-determining step during FRAP recovery to allow the reliable formulation of simplified mathematical models and estimate  $k_{\text{OFF}}$ . Together, this information allows us to estimate  $k_{\text{ON}}$ .

## MATERIALS AND METHODS

### Cell Culture

NIH3T3 cells were cultured in DMEM supplemented with 10% fetal bovine serum. GFP-Histone H1.1 was kindly provided by Prof. Mike Hendzel. Transfections were performed using Superfect (Qiagen). For FRAP experiments, cells were grown on 40 mm glass coverslips and transferred to a FCS2 live cell chamber (Bioprotechs) mounted on a Leica SP laser scanning confocal microscope with objective heater. The temperature was maintained at 37°C. In some experiments, the cells were fixed with 4% formaldehyde/0.1% glutaraldehyde in permeabilization buffer (20 mM HEPES, pH 7.3; 110 mM potassium acetate; 2 mM magnesium acetate) for 45 min prior to transferring them to the microscope.

### Fluorescence Recovery After Photobleaching

Images of the nucleus were scanned before and after bleaching at low laser power (10% of

full power) on the Leica SP laser scanning confocal microscope. Cells were chosen randomly with respect to protein expression level, nuclear shape and size; 15–20 cells were analyzed for each condition. Routinely, 2 images were taken before and 20–30 images after the bleach at intervals of 20 s depending on the time of recovery. To bleach all fluorescent EGFP-proteins in the nucleus, maximal laser power (100% of full power) was applied to the region of interest for 3 s. Leica confocal software (version 2) was used to measure the intensity of fluorescence in the bleached area and in the whole nucleus for the whole stack of images. For analysis, these data were first corrected for loss in bleaching during image acquisition as follows: at any given time  $t$ ,  $D = (I - I_b)/(I_w - I_b)$  is the corrected data where  $I$  is the average fluorescent intensity in the bleached spot,  $I_b$  and  $I_w$  are the background and whole nucleus average intensities; all at time  $t$ . To plot Figure 2A,  $D$  was normalized to the amount photobleached, that is,  $D(t)/(D(0) - D(t_b))$  where  $t_b$  is the time at which bleaching was performed. To plot Figure 2B, the data was normalized as  $\frac{D(t) - D(t_b)}{D(t_{\infty}) - D(t_b)}$ ,  $t \geq t_b$ ; this was also fit to an exponential function  $1 - e^{-k_{OFF}t}$  for determining  $k_{OFF}$ . Fitting was performed using Matlab v6.5 with the `lsqcurvefit` function. Statistical analysis was performed using the Student's  $t$ -test ( $t$ -test 2 function in Matlab v6.5).

## RESULTS

### Determination of the Rate-Limiting Step

To calculate the rate constants for binding ( $k_{ON}$ ) and unbinding ( $k_{OFF}$ ) for a protein within living cells, a mathematical model must be formulated that faithfully represents the physical process. This demands that the rate-limiting step that governs recovery during FRAP analysis be correctly identified. If the fluorescence recovery measured during FRAP in cells is diffusion-limited, then the characteristic recovery time (e.g., time required for 50% fluorescence recovery,  $t_{1/2}$ ) is proportional to the area of the photobleached spot [Lele et al., 2004; Sprague et al., 2004].

To identify the rate-limiting step for histone H1 binding to chromatin, we carried out FRAP experiments in NIH3T3 cells expressing EGFP-histone H1 which localized throughout the nucleus in a diffuse pattern (Fig. 1), as previously described [Th'ng et al., 2005]. We carried out FRAP experiments by either photobleaching a small circular spot ( $16 \mu\text{m}^2$ ) in the nucleus (Fig. 1A), or exposing more than half of the nuclear cross-sectional area to laser light (Fig. 1B). In both cases, complete fluorescence recovery due to diffusion of fluorescent GFP-histone H1 from non-irradiated regions into the bleached zone, and binding to chromatin at this site, occurred in approximately 3 min.

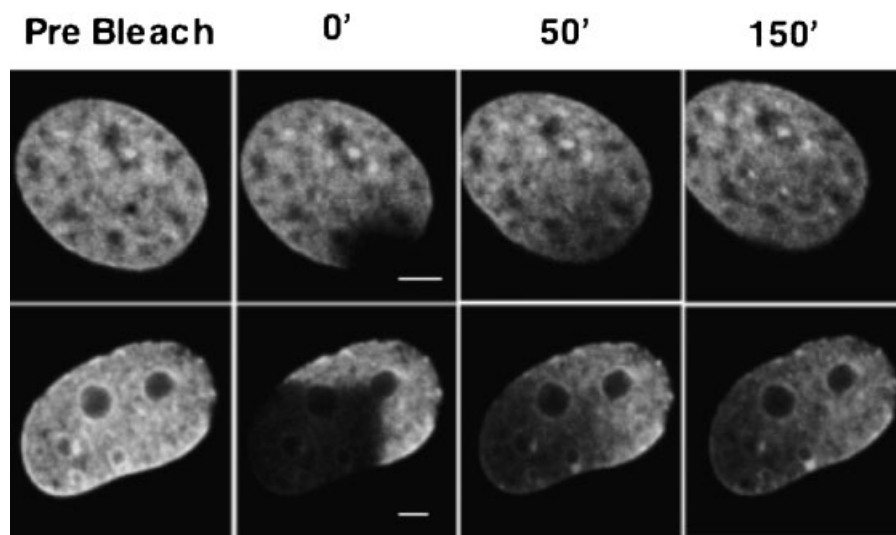


**Fig. 1.** FRAP recovery of GFP-Histone H1 is insensitive to spot size. Fluorescence confocal microscopic images recorded during FRAP analysis of NIH 3T3 cells expressing GFP-histone H1 in which small (top;  $16 \mu\text{m}^2$ ) or large (bottom;  $125 \mu\text{m}^2$ ) areas of the nucleus were photobleached (bar,  $3 \mu\text{m}$ ).

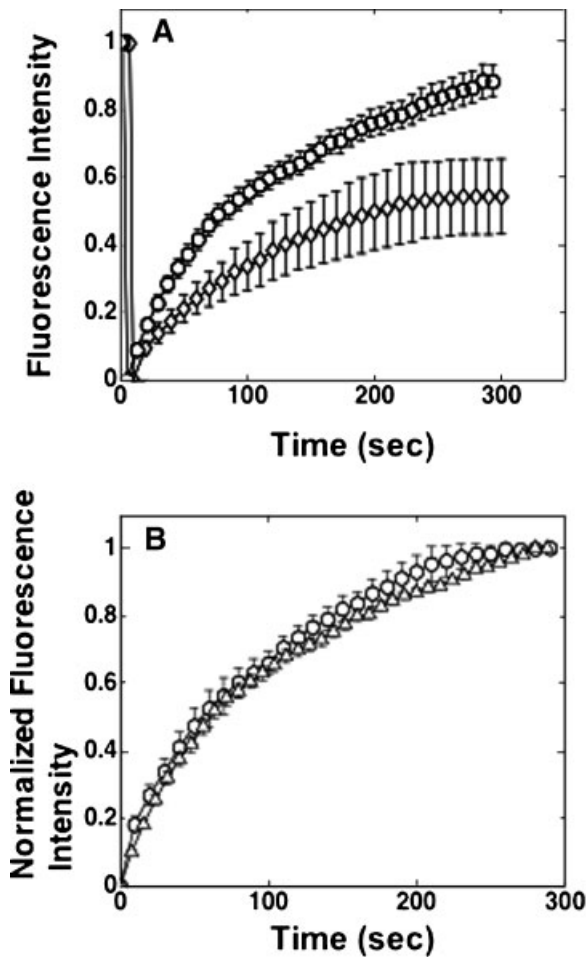


**Fig. 2.** FRAP recovery curves of GFP-histone H1 are not sensitive to the size of the photobleached spot. **A:** Recovery GFP-histone H1 fluorescence intensity within a photobleached spot in cells exposed to the small (open circles) or large (open diamonds) laser spot size (error bars indicate SEM). Note that the fluorescence intensity recovers less for the larger bleach spot. **B:** Recovery curve corresponding to the data in (A) normalized for differences in total fluorescence recovery, such that the fluorescence intensity in the bleached spot is zero immediately after laser exposure, and one after complete recovery. Note that this time-dependent recovery is similar for the small (open circle) and large (open triangles) spot sizes.

Analysis of these results revealed that the final level of recovered fluorescence intensity at steady state was significantly lower when the larger area was photobleached due to a greater loss of total fluorescence intensity (Fig. 2A). However, when the data were normalized for the total amount of fluorescent recovery in each cell (see Materials and Methods), we found that the temporal dependence of the normalized fluorescence recovery was insensitive to the size of the photobleached spot (Fig. 2B). In other

words, although the total level of fluorescence intensity recovered was less for the larger bleach spot size, the rate of recovery of fluorescence remained unchanged (Fig. 2B). Importantly, this finding indicates that diffusion did *not* play a significant role in the recovery, because if it did, then the rate of recovery would depend directly on the spot size. Thus, the fluorescence recovery of GFP-histone H1 during FRAP in these cells is limited by binding and unbinding kinetics, rather than diffusion [Lele et al., 2004; Sprague et al., 2004]. Although the rate of recovery during FRAP may be sensitive to spatial location of the photobleached spot, measurements were performed without regard to spatial location, and hence they represent an average value measured over different spatial domains.

GFP-histone H1 exists in the nucleus in two states: chromatin-bound or freely diffusing. Because FRAP recovery of GFP-histone H1 is not diffusion limited (Figs. 1 and 2), the bound histone protein must exchange with the free protein much more slowly than free histone can diffuse. This is expected because the molecular weight of GFP-histone H1 (~50 kDa) is not significantly different from that of unconjugated GFP (~27 kDa), which diffuses very rapidly inside the nucleus. A mutant GFP-histone created by the deletion of the globular or C-terminal domain of the histone molecule which mediates DNA binding has been shown to diffuse as rapidly as free GFP [Lever et al., 2000; Hendzel et al., 2004]. Thus, our FRAP data indicate that non-specific binding of GFP-histone H1 to chromatin or other insoluble nuclear scaffolds is insignificant in these cells. These observations, taken together with the results in Figures 1 and 2, suggest that free GFP-histone H1 diffuses across the entire nuclear space in a time scale of less than a second, whereas chromatin-bound GFP-histone H1 exchanges with the nucleoplasmic pool over a much slower time scale.

The FRAP recovery dynamics for GFP histone H1 are therefore indicative of a “reaction-dominant” mechanism in which the binding and unbinding rate are much faster than the rate of diffusion as represented by the Damköhler number  $k_{ON}w^2/D_H \ll 1$  [Lele et al., 2004; Sprague et al., 2004] where  $w$  is the size of the photobleached spot and  $D_H$  is the diffusion coefficient of GFP histone H1. Under these conditions, the rate of FRAP recovery is determined

by a time scale of  $1/k_{\text{OFF}}$  (see Appendix), thus allowing the direct determination of  $k_{\text{OFF}}$  for histone H1 binding to DNA in the living nucleus from FRAP [Bulinski et al., 2001; Lele et al., 2004].

#### Estimation of the Ratio of Free Versus bound Protein

To determine  $k_{\text{ON}}$ , it is necessary to first estimate the free versus bound concentration of protein in the nucleus. To accomplish this, we measured the level of nuclear fluorescence intensity for GFP-histone before and after cells were extracted in buffer containing 0.5% Triton-X-100 to remove lipids and soluble proteins. The level of fluorescence intensity after extraction reflects the concentration of the bound protein, and the lost fluorescence intensity corresponds to the concentration of free protein. On average, 25% of the fluorescence signal was lost during the extraction process indicating that the ratio of free to bound histone H1 was approximately 1:3. However, in addition to freely diffusing histone molecules, some bound histone H1 may also be removed due to unbinding and exit from the nucleus during the 4 min extraction process. Thus, this detergent-extraction experiment may overestimate the percentage of free histone H1 in living cells.

To more accurately estimate this ratio, we developed a method to rapidly photobleach all the freely diffusing GFP-histone H1 molecules in the nucleus without losing the bound form of the molecule, and to quantify the resulting loss in fluorescence. We took advantage of the fact that free GFP-histone H1 diffuses very rapidly (as fast as free GFP). When we exposed a small circular region (4  $\mu\text{m}$  diameter) of the nucleus of a cell expressing GFP alone to laser light for an extended time (3 s), all of the rapidly diffusing free GFP molecules were free to enter the light path; this resulted in bleaching of the *entire* pool of freely diffusing GFP-labeled molecules as indicated by loss of more than 80% of the nuclear fluorescence intensity, without affecting cytoplasmic staining levels (Fig. 3A,B).

Given that free GFP and GFP-histone H1 have similar mobilities, we reasoned that a similar photobleaching experiment with histone H1 will bleach all the freely diffusing protein throughout the nuclear space while leaving the bound fluorescent protein outside the photobleached spot unbleached. When we photobleached GFP-histone H1 in the nucleus

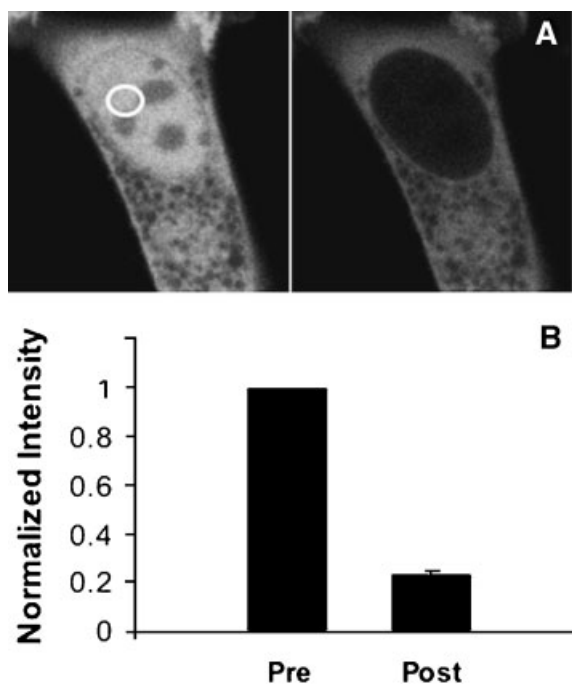


**Fig. 3.** Extended exposure of a small region of the nucleus to laser light completely photobleaches the entire nuclear pool of freely diffusing GFP. **A:** Fluorescence microscopic images of a cell expressing free GFP before (left) and after (right) 3-s exposure to a small spot (white circle) of laser light. **B:** Graph of the measured changes in total nuclear fluorescence intensity before (pre) and after (post) irradiation showing that this exposure resulted in nearly 80% elimination of nuclear GFP fluorescence.

at a fixed spot in a similar manner (Fig. 4A), the fluorescence intensity in non-irradiated regions of nucleus surrounding the spot decreased by over 7% ( $P < 0.00001$ ) (Fig. 4B).

This lost fraction that appears to be attributable to free GFP-histone H1 is much smaller than the 25% we measured using the Triton X-100 permeabilization technique. To explore this further, similar photobleaching experiments were performed in cells that were fixed with a mixture of paraformaldehyde and glutaraldehyde to irreversibly cross-link GFP-Histone H1 to chromatin and other nuclear structures and thereby prevent diffusion. There was no decrease in nuclear fluorescence outside the bleach zone when these fixed cells were irradiated in a similar manner (Fig. 4B). These data confirm that the decrease of fluorescence intensity measured in regions of the nucleus outside the photobleached zone was indeed due to freely diffusing GFP-histone molecules.

When diffusion is much faster than binding and unbinding, the normalized FRAP recovery data yield  $k_{\text{OFF}}$  (see Appendix). Fitting normalized

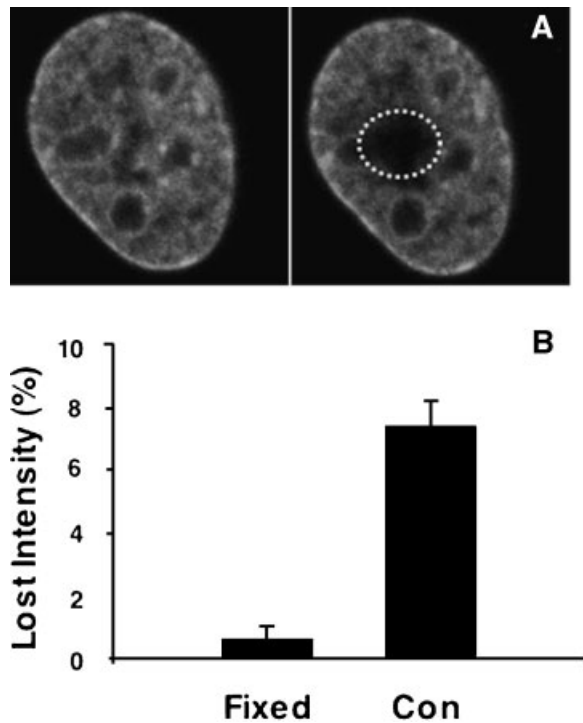


**Fig. 4.** Loss of fluorescence intensity of GFP-histone H1 from areas outside the photobleached spot is insignificant in fixed cells. **A:** Fluorescence microscopic images before (left) or after (right) a portion of the nucleus expressing GFP-histone H1 was exposed to 3 s of laser light (dashed white circle) in living cells. **B:** Graph showing the loss of fluorescence intensity (%) in regions surrounding the photobleached spot in control (Con) versus fixed (Fixed) cells.

GFP-Histone H1 FRAP recovery curves to the formula  $1 - e^{-k_{\text{OFF}}t}$ , we estimated that  $k_{\text{OFF}} = 0.0131/\text{s}$ . Because freely diffusing GFP was not bleached completely ( $\sim 80\%$ ) after the 3 s laser exposure, the free to bound ratio measured in Figure 4 was corrected for this difference. We obtained the ratio of  $k_{\text{OFF}}/k_{\text{ON}} = K = 0.096$  ( $K$  is the equilibrium constant) which indicates that  $k_{\text{ON}} = 0.14/\text{s}$  for histone H1 in the nuclei of these living cells.

## DISCUSSION

We have developed a method to determine  $k_{\text{ON}}$  and  $k_{\text{OFF}}$  for the binding of histone H1 to chromatin in living cells using photobleaching methods and mathematical modeling. First, we demonstrated that GFP-histone H1 binding is not limited by diffusion and thus, we were able to directly determine the unbinding rate constant  $k_{\text{OFF}}$  from FRAP experiments. We then developed a modified photobleaching method whereby we can estimate the proportion of free

to bound histone H1 molecules within nuclei, which is equal to  $k_{\text{OFF}}/k_{\text{ON}}$  (see appendix for mathematical analysis). Together, these measurements allowed us to estimate the binding constant  $k_{\text{ON}}$  of histone H1 in living cells. It should be noted that the normalized recovery time we observed during FRAP for GFP-histone-H1 is slower than that previously observed [Th'ng et al., 2005]; however, this is likely due to differences in cell type as has been observed for other nuclear proteins [Kruhlak et al., 2000].

Histone binding and unbinding rate constants are direct measures of protein interactions that can be regulated biologically. For example, linker histone release from DNA is a regulated phenomenon in the mechanism of gene activation [Zlatanova et al., 2000]. Compared to nucleosomal core histones, fewer reported postranslational modifications and protein-binding partners have been reported for histone H1 variants; however, histone H1 can be serine phosphorylated. FRAP experiments with *Tetrahymena* show that mutants of histone H1 engineered to mimic the charge distributions of either the phosphorylated or unphosphorylated forms have different rates of exchange on chromatin [Dou et al., 2002]. Cyclin/CDK phosphorylation was shown to govern histone H1 exchange kinetics as measured by FRAP in mammalian cells [Contreras et al., 2003].

Histone H1 also binds to heterochromatin protein 1 (HP1) during heterochromatin formation [Nielsen et al., 2001] and this interaction could stabilize condensed chromatin structures. Additionally, histone H1 binds barrier-to-auto-integration factor (BAF) in vitro [Montes de Oca et al., 2005], an interaction that could also be important in the spatial organization of chromatin at the nuclear periphery. If all these interactions are biologically significant we might expect local alterations in histone H1 binding and unbinding rates that could, with appropriate biological manipulations, be probed with the methods we present here. Additionally, different histone H1 subtypes may have different binding kinetics because they recover differently during FRAP [Th'ng et al., 2005]. Thus, the measurement of histone H1 rate constants by FRAP could be an important tool for probing fundamental biological regulatory mechanisms underlying the function of this critical chromatin protein in living cells.

There are certain assumptions underlying our analysis that are important for the interpretation of binding constants. All histone H1 binding sites are assumed to be identical. As there is no consensus DNA sequence for histone H1 binding, it is likely that the binding constants that we measured are an average for all sites. There are also some caveats before this method can be generalized to other nuclear proteins that exist in bound and freely diffusing forms. First, when we irradiated a small region of the nucleus for 3 s to bleach all free diffusing proteins, it is possible that some of the bound fluorescent protein unbinds, diffuses into this region, and hence, also gets bleached during the experiment; in this case, the free to bound ratio may be overestimated. The interconversion between fluorescent bound and free protein in unbleached areas is determined by the rate constant  $k_{ON}$  (see Equation (7) in the Appendix). Thus, this analysis will be most accurate under conditions in which the binding rate is much slower than diffusion so that the cross talk between bound and freely diffusing protein does not play a significant role. This can be confirmed, as we did here, by showing that the FRAP recovery is insensitive to spot size, as shown in Figures 1 and 2.

The  $k_{ON}$  for histone H1 measured in this paper is the multiplicative product of the binding rate constant  $k_{ON}^*$  and the concentration of protein binding sites available  $S$  (see binding rate expression in the Appendix). Thus, any changes that are measured in  $k_{ON}$  could arise from a change in either the rate constant  $k_{ON}^*$  (indicating changes in binding energy landscapes) or the number of available binding sites. A separate assay would be necessary to distinguish between these two effects.

In conclusion, we have developed a simple method to estimate  $k_{OFF}$  and  $k_{ON}$  for proteins that bind to insoluble nuclear structures when diffusion is not rate limiting in FRAP experiments. To accomplish this, the rate-limiting step must be identified and we demonstrated that this can be done experimentally by carrying out FRAP experiments in which the spot size areas are varied. If diffusion is very fast compared to binding and unbinding, the fractional amount of freely diffusing protein can be determined by bleaching a small stationary spot in the nucleus for an extended time and exposing all rapidly diffusing free molecules to the fixed laser light. This ratio of free to bound

protein yields  $k_{OFF}/k_{ON}$  which together with an independent determination of  $k_{OFF}$  with FRAP allows the estimation of  $k_{ON}$ . This method can be readily applied to quantify binding interactions in living cells for all those proteins where binding and unbinding are significantly faster than diffusion, and thus may be useful for many areas of cell biological research.

## ACKNOWLEDGMENTS

Prof. Mike Hendzel's kind gift of GFP-histone H1.1 is gratefully acknowledged. These studies were supported by grants from NIH (CA-45548) to D.E.I., and an NSF grant (DMR-0213805 to Harvard University in support of its Materials Research Science Engineering Center). J.A.N. acknowledges funding from the American Cancer Society (RSG 99-262-04) and the National Cancer Institutes (PO1 CA82834).

## APPENDIX

### Kinetic Rate Laws for Histone H1

Let free histone H1 molecules be denoted by  $H$ , and available binding sites by  $S$ , then we can denote the binding process by



where  $HS$  denotes bound histone molecules where  $k_{ON}$  and  $k_{OFF}$  denote rate constants for the forward and reverse steps in Equation (1). The rate of binding will depend on the concentration of free histone molecules as well as the number of available binding sites. Thus, the rate of binding is given by (e.g., see the derivation of the Langmuir isotherm; [Hiemenz and Rajagopalan, 1997])

$$\begin{aligned} r_{ON} &= k_{ON}^* \\ &\times (\text{free histone}) \\ &\times (\text{available binding sites}) \\ &= k_{ON}^* CS \end{aligned}$$

where  $C$  is the concentration of freely diffusing histone molecules and  $S$  is the concentration of available binding sites. The rate of the reverse step in (1) is determined purely by the number of bound histone molecules, thus  $r_{OFF} = k_{OFF} \times (\text{bound histone}) = k_{OFF} \hat{C}$  where  $\hat{C}$  is the concentration of bound histone.

### Mathematical Model

We assume that there is no spatial gradient during fluorescence recovery; this assumption was verified using the method developed in Figure (1). Let the area of photobleach be  $A_0$  and the total nuclear area be  $A$ . Before photobleaching, let the concentration of fluorescent free protein be  $C_{F,0}$  and that of fluorescent bound protein be  $\hat{C}_{F,0}$ . Then on photobleaching, there is a loss of  $\beta C_{F,0}A + (1 - \alpha)\hat{C}_{F,0}A_0$  where  $\alpha\hat{C}_{F,0}A_0$  is the fluorescence in the photobleached spot immediately after bleach (different from zero) and  $\beta C_{F,0}A$  is the extent of bleaching of the freely diffusing protein throughout the nucleus (for example,  $\beta = 0.8$  for our experiments (Fig. 3)). Let the concentration of fluorescent bound protein in the non-bleached areas be  $\hat{C}_{F,N-S}$  and that of fluorescent free protein be  $C_F$ . Since photobleaching does not disturb local equilibrium in any way, but merely makes a fraction of the fluorescent molecules invisible, we have the constraint

$$C_F(t)A + \hat{C}_{F,S}(t)A_0 + \hat{C}_{F,N-S}(t)(A - A_0) = \hat{C}_{F,0}(\alpha A_0 + A - A_0) + C_{F,0}\beta A \quad (2)$$

or

$$\frac{dC_F}{dt} + \frac{d\hat{C}_{F,S}}{dt} \frac{A_0}{A} + \frac{d\hat{C}_{F,N-S}}{dt} \frac{A - A_0}{A} = 0 \quad (3)$$

The mass balance during recovery after photobleaching is

$$\frac{d\hat{C}_{F,N-S}}{dt} = k_{ON}C_F - k_{OFF}\hat{C}_{F,N-S} \text{ and} \quad (4a)$$

$$\frac{d\hat{C}_{F,S}}{dt} = k_{ON}C_F - k_{OFF}\hat{C}_{F,S} \text{ where } k_{ON} = k_{ON}^*S \quad (4b)$$

From the constraint, we get

$$\begin{aligned} \frac{dC_F}{dt} &= -\frac{d\hat{C}_{F,S}}{dt} \frac{A_0}{A} - \frac{d\hat{C}_{F,N-S}}{dt} \frac{A - A_0}{A} \\ &= \left( k_{OFF}\hat{C}_{F,S} - k_{ON}C_F \right) \frac{A_0}{A} \\ &\quad + \left( k_{OFF}\hat{C}_{F,N-S} - k_{ON}C_F \right) \frac{A - A_0}{A} \\ &= k_{OFF}\hat{C}_{F,S} \frac{A_0}{A} + k_{OFF}\hat{C}_{F,N-S} \frac{A - A_0}{A} \\ &\quad - k_{ON}C_F \end{aligned} \quad (5)$$

Before the photobleaching experiment, if the bound and free protein are assumed to be at

steady state, then  $\hat{C}_{F,0} = \frac{k_{ON}^*}{k_{OFF}} C_{F,0} = \frac{1}{K} C_{F,0}$ . Defining,  $c_F \equiv \frac{C_F}{C_{F,0}}$ ,  $\hat{c}_{F,S} \equiv \frac{K\hat{C}_{F,S}}{C_{F,0}}$  and  $\hat{c}_{F,N-S} \equiv \frac{K\hat{C}_{F,N-S}}{C_{F,0}}$ , Equations (4) and (5) become

$$\frac{d\hat{c}_{F,N-S}}{dt} = k_{OFF}(c_F - \hat{c}_{F,N-S}) \quad (6a)$$

$$\frac{d\hat{c}_{F,S}}{dt} = k_{OFF}(c_F - \hat{c}_{F,S}) \quad (6b)$$

$$\frac{dc_F}{dt} = k_{ON} \left( \hat{c}_{F,S} \frac{A_0}{A} + \hat{c}_{F,N-S} \frac{A - A_0}{A} - c_F \right) \quad (7)$$

From Equation (7), it is immediately apparent that the free protein recovers on a time scale of  $1/k_{ON}$ . FRAP does not distinguish between bound and freely diffusing protein, the measurement is of the total fluorescence due to freely diffusing and bound protein. We add the differential equations describing free and bound protein (using Equations (4) and (5)) in the photobleached spot to get

$$\begin{aligned} \frac{d}{dt} (C_F + \hat{C}_{F,S}) \\ = k_{OFF} \left( \hat{C}_{F,S} \frac{A_0}{A} + \hat{C}_{F,N-S} \frac{A - A_0}{A} - \hat{C}_{F,S} \right) \end{aligned} \quad (8)$$

From this equation, it is clear that the time scale governing the sum of freely diffusing and bound protein concentrations is  $k_{OFF}$  and does not involve  $k_{ON}$ . Substituting for  $\hat{C}_{F,N-S}$  from Equation (2), Equation (8) becomes

$$\begin{aligned} \frac{d}{dt} (C_F + \hat{C}_{F,S}) \\ = k_{OFF} \left( \hat{C}_{F,0} \left( \alpha \frac{A_0}{A} + \frac{A - A_0}{A} \right) + \beta C_{F,0} \right) \\ - k_{OFF} (C_F + \hat{C}_{F,S}) \end{aligned} \quad (9)$$

A popular normalization strategy followed in the literature is to calculate the following ratio  $F(t) = \frac{(C_F(t) + \hat{C}_{F,S}(t)) - (C_F(t=0) + \hat{C}_{F,S}(t=0))}{(C_F(t \rightarrow \infty) + \hat{C}_{F,S}(t \rightarrow \infty)) - (C_F(t=0) + \hat{C}_{F,S}(t=0))}$ . The solution to Equation (9) in terms of this ratio is  $F(t) = 1 - e^{-k_{OFF}t}$ . This indicates that normalized FRAP data under reaction dominant conditions only depends on  $k_{OFF}$  and is independent of other parameters like  $k_{ON}$ ,  $\alpha$ , and  $\beta$ .

### REFERENCES

- Bilinski JC, Odde DJ, Howell BJ, Salmon TD, Waterman-Storer CM. 2001. Rapid dynamics of the microtubule binding of ensconsin in vivo. *J Cell Sci* 114:3885-3897.

- Carrero G, McDonald D, Crawford E, de Vries G, Hendzel M. 2003. Using FRAP and mathematical modeling to determine the in vivo kinetics of nuclear proteins. *Methods* 29:14–28.
- Contreras A, Hale TK, Stenoien DL, Rosen JM, Mancini MA, Herrera RF. 2003. The dynamic mobility of histone H1 is regulated by cyclin/CDK phosphorylation. *Mol Cell Biol* 23(23):8626–8636.
- Dou Y, Bowen J, Liu Y, Gorovsky MA. 2002. Phosphorylation and an ATP-dependent process increase the dynamic exchange of H1 in chromatin. *J Cell Biol* 158:1161–1170.
- Hendzel MJ, Lever MA, Crawford E, Th'ng JP. 2004. The C-terminal domain is the primary determinant of histone H1 binding to chromatin in vivo. *J Biol Chem* 279:20028–20034.
- Hiemenz PC, Rajagopalan R. 1997. Principles of colloid and surface chemistry. Marcel Dekker.
- Hinojos CA, Sharp ZD, Mancini MA. 2005. Molecular dynamics and nuclear receptor function. *Trends Endocrinol Metab* 16(1):12–18.
- Imbalzano AN, Xiao H. 2004. Functional properties of ATP-dependent chromatin remodeling enzymes. *Adv Protein Chem* 67:157–179.
- Ingber DE. 1993. The riddle of morphogenesis: A question of solution chemistry or molecular cell engineering? *Cell* 75:1249–1252.
- Karpova TS, Chen TY, Sprague BL, McNally JG. 2004. Dynamic interactions of a transcription factor with DNA are accelerated by a chromatin remodeler. *EMBO Rep* 5:1064–1070.
- Kaufman EN, Jain RK. 1990. Quantification of transport and binding parameters using fluorescence recovery after photobleaching. *Biophys J* 58:873–885.
- Kaufman EN, Jain RK. 1991. Measurement of mass transport and reaction parameters in bulk solution using photobleaching. *Biophys J* 60:596–608.
- Koppel D, Sheetz M. 1983. A localized pattern photobleaching method for the concurrent analysis of rapid and slow diffusion processes. *Biophys J* 43:175–181.
- Kruhlak MJ, Lever MA, Fischle W, Verdin E, Bazett-Jones DP, Hendzel MJ. 2000. Reduced mobility of the alternate splicing factor (ASF) through the nucleoplasm and steady state speckle compartments. *J Cell Biol* 150:41–51.
- Lele T, Ingber D. 2006. A mathematical model to determine molecular kinetic rate constants under non-steady state conditions using fluorescence recovery after photobleaching (FRAP). *Biophys Chem* 120:32–35.
- Lele TP, Oh P, Nickerson J, Ingber D. 2004. An improved mathematical approach for determination of molecular kinetics in living Cells with FRAP. *Mechanics and Chemistry of Biosystems* 1:181–190.
- Lele T, Pendse J, Kumar S, Salanga M, Karavitis J, Ingber D. 2005. Mechanical forces alter zyxin unbinding kinetics within focal adhesions of living cells. *J Cellular Physiology* In press.
- Lever MA, Th'ng JP, Sun X, Hendzel MJ. 2000. Rapid exchange of histone H1.1 on chromatin in living human cells. *Nature* 408:873–876.
- Luger K, Mader AW, Richmond RK, Sargent DF, Richmond TJ. 1997. Crystal structure of the nucleosome core particle at 2.8 Å resolution. *Nature* 389:251–260.
- Mamoon NM, Song Y, Wellman SE. 2005. Binding of histone H1 to DNA is described by an allosteric model. *Biopolymers* 77:9–17.
- Montes de Oca R, Lee KK, Wilson KL. 2005. Binding of barrier-to-autointegration factor (BAF) to histone H3 and selected linker histones including H1.1. *J Biol Chem*
- Nickerson J. 2001. Experimental observations of a nuclear matrix. *J Cell Sci* 114:463–474.
- Nielsen AL, Oulad-Abdelghani M, Ortiz JA, Remboutsika E, Chambon P, Losson R. 2001. Heterochromatin formation in mammalian cells: Interaction between histones and HP1 proteins. *Mol Cell* 7:729–739.
- Olins AL, Olins DE. 1974. Spheroid chromatin units (v bodies). *Science* 183:330–332.
- Phair R, Misteli T. 2000. High mobility of proteins in the mammalian cell nucleus. *Nature* 404:604–609.
- Phair R, Misteli T. 2001. Kinetic modelling approaches to in vivo imaging. *Nat Rev Mol Cell Biol* 2:898–907.
- Phair RD, Gorski SA, Misteli T. 2004a. Measurement of dynamic protein binding to chromatin in vivo, using photobleaching microscopy. *Methods Enzymol* 375:393–414.
- Phair RD, Scaffidi P, Elbi C, Vecerova J, Dey A, Ozato K, Brown DT, Hager G, Bustin M, Misteli T. 2004b. Global nature of dynamic protein-chromatin interactions in vivo: Three-dimensional genome scanning and dynamic interaction networks of chromatin proteins. *Mol Cell Biol* 24:6393–6402.
- Presley J, Ward T, Pfeifer A, Siggia E, Phair R, Lippincott-Schwartz J. 2002. Dissection of COPI and Arf1 dynamics in vivo and role in Golgi membrane transport. *Nature* 417:187–193.
- Richmond TJ, Finch JT, Rushton B, Rhodes D, Klug A. 1984. Structure of the nucleosome core particle at 7 Å resolution. *Nature* 311:532–537.
- Sprague BL, McNally JG. 2005. FRAP analysis of binding: Proper and fitting. *Trends Cell Biol* 15:84–91.
- Sprague BL, Pego RL, Stavreva DA, McNally JG. 2004. Analysis of binding reactions by fluorescence recovery after photobleaching. *Biophys J* 86:3473–3495.
- Stenoien DL, Nye AC, Mancini MG, Patel K, Dutertre M, O'Malley BW, Smith CL, Belmont AS, Mancini MA. 2001. Ligand-mediated assembly and real-time cellular dynamics of estrogen receptor alpha-coactivator complexes in living cells. *Mol Cell Biol* 21(13):4404–4412.
- Stenoien DL, Mielke M, Mancini MA. 2002. Intracellular ataxin1 inclusions contain both fast and slow-exchanging components. *Nat Cell Biol* 4(10):806–810.
- Tardy Y, McGrath J, Hartwig J, Dewey C. 1995. Interpreting photoactivated fluorescence microscopy measurements of steady-state actin dynamics. *Biophys J* 69:1674–1682.
- Th'ng JP, Sung R, Ye M, Hendzel MJ. 2005. H1 family histones in the nucleus. Control of binding and localization by the C-terminal domain. *J Biol Chem* 280:27809–27814.
- Travers A. 1999. The location of the linker histone on the nucleosome. *Trends Biochem Sci* 24:4–7.
- Wolffe A. 1998. Chromatin: Structure and function. London: Academic Press.
- Zink D, Fischer AH, Nickerson JA. 2004. Nuclear structure in cancer cells. *Nat Rev Cancer* 4:677–687.
- Zlatanova J, Caiafa P, Van Holde K. 2000. Linker histone binding and displacement: Versatile mechanism for transcriptional regulation. *FASEB J* 14:1697–1704.